processes

MDPI

Article

Antibacterial Effect of Polyvinyl Alcohol/Biochar–Nano Silver/Sodium Alginate Gel Beads

Licheng Xie [1], Zhichao Zhang [1,2] and Yucai He [3,*]

[1] Changzhou University Huaide College, Jingjiang 214500, China; lichengxie@smail.cczu.edu.cn (L.X.); zhangzhichao9088@163.com (Z.Z.)
[2] School of Chemistry and Chemical Engineering, Guangxi University, Nanning 530004, China
[3] School of Pharmacy, Changzhou University, Changzhou 213164, China
* Correspondence: yucaihe@cczu.edu.cn

Abstract: To date, biochar bacteriostatic material has attracted much attention from researchers. The compact porous structure of fish-scale biochar provides good application prospects. In this study, silver-carrying biochar–polyvinyl alcohol–alginate gel beads (C/PVA/SA) were designed for suppressing bacteria. The biochar was loaded with nano silver particles as the filler, alginate as the substrate, and polyvinyl alcohol (PVA) as the additive to enhance the mechanical properties. The composite gel beads were characterized using Fourier-transform infrared spectrometry (FT-IR). The results indicated that adjusting the PVA concentration could retain the bacteriostatic performance of the gel beads in different pH value solutions. It was found that C/PVA/SA gel beads had a strong inhibitory effect on *Escherichia coli*, *Staphylococcus aureus*, and *Pseudomonas aeruginosa*. After ten consecutive antibacterial tests, the antibacterial rate remained high (above 99%) for 15 days. The adhesive effect of SA and PVA resulted in a tight spatial structure of the gel beads. The C/PVA/SA gel composition could effectively prevent water loss and enhance the shrinkage ability of the gel beads. The good degradation performance of C/PVA/SA was also in line with the concept of environmental protection. In general, the C/PVA/SA gel beads showed high potential for application in the treatment of microbial contamination and environmental protection.

Keywords: antibacterial ability; fish-scale biochar; nanosilver antibacterial composite

Citation: Xie, L.; Zhang, Z.; He, Y. Antibacterial Effect of Polyvinyl Alcohol/Biochar–Nano Silver/Sodium Alginate Gel Beads. *Processes* **2023**, *11*, 2330. https://doi.org/10.3390/pr11082330

Academic Editor: Pavel Mokrejš

Received: 22 June 2023
Revised: 18 July 2023
Accepted: 31 July 2023
Published: 3 August 2023

1. Introduction

With accelerated industrial production and complex life activity, microbial pollution arises frequently and severely, which could seriously endanger human health [1]. Polluted water can become a medium for spreading diseases and pose a severe threat to human health [2]. It is crucial to treat drinking water with safe bacteriostatic materials with an efficient approach [3]. Considering the different water qualities, it is urgent to prepare a bacteriostatic material that can adapt to a series of water conditions and has good bacteriostatic properties. Biochar is a readily available and cheap biobased material, which is extensively utilized as a carrier of nano-metal ions in the antibacterial field [4]. Fish are reported to produce large amounts of waste during processing, with about 80 million tons of fish waste annually produced globally [5]. Fish scales are rich in protein, calcium, collagen, fat, and minerals. However, the disposal of fish scale waste generates high chemical and biological oxygen demand and contains some pathogenic bacteria that pose an obvious environmental hazard [6]. It is of great interest to prepare the porous surface structure of fish-scale biochar. It is well known that silver is often utilized in antibacterial composites because of its broad spectrum and good durability [7]. Silver nanoparticles (AgNPs) have been found to have high antibacterial properties [8], which can damage cell membranes through the exchange of negative and positive charges, resulting in material leakage in the cell [9]. Biochar-based composite-loaded silver has good antibacterial properties [10].

However, the small particle size of silver-carrying biochar is not easy to recycle, resulting in material loss. The preparation of antibacterial composite materials with ease of use and rapid recovery has gained more and more attention.

Sodium alginate (SA) is a by-product of iodine and mannitol extracted from some brown algae [11]. It is one kind of polysaccharide that can form a hydrogel network with most divalent metal ions [12]. SA is widely utilized to immobilize bacteria, due to its sole hydrogel network properties [13]. Recently, alginate saline gel beads have gained considerable interest in the adsorption process because of their rich mesoporous and macroscopic structures, which can be processed into desirable sizes and shapes [14]. However, alginate–saline gel beads have poor mechanical properties [15], which limits their application. Thus, it is necessary to supplement organic or inorganic fillers into the gel bead preparation system, modify their physicochemical properties, enhance their mechanical strength, and adapt the bead materials to various performance environments. Polyvinyl alcohol (PVA) is a eco-friendly, water-soluble, biodegradable, non-toxic, and biocompatible biopolymer gel [16]. It is an important chemical raw material for manufacturing emulsifiers, coatings, and adhesives. PVA has a hydrophilic property and is also often utilized as a support for the immobilization of bacteria [17]. However, the immobilized materials with PVA as the main component cannot be repeatedly reused for a long performance time [18]. PVA and SA can generate stable immobilized carriers via an adhesive interaction [19]. After SA and PVA are immersed in water, the alginate anion formed by electrolysis can attach to the PVA surface. After the SA/PVA composite solution is immersed in a $CaCl_2$ solution, the Ca^{2+} may attract the alginate anion via electrostatic interaction and develop SA/PVA gel beads [20]. The pores inside the SA/PVA gel beads are dense, and the biological silver-loaded carbon particles can be more easily loaded on the adhesive structure. The internal network structure of PVA/SA gel beads, which have high mechanical strength and chemostability after crosslinking, provides a carrier for antibacterial silver-containing biochar in water [21].

In this work, C/PVA/SA gel beads were prepared using silver-loaded fish-scale biochar as the filler, SA as the carrier, and PVA as the reinforcer. The silver-loaded fish-scale biochar was denoted as C-Ag. The preparation of the C-Ag not only developed a new bacteriostatic material but also created a new idea for the reuse of fish-scale waste. The encapsulation structure of gel beads could solve the problems of the separation and recovery of silver-loaded biochar [22]. The C/PVA/SA gel beads had strong stability, a high swelling performance, a small volume after preparation, and maintained excellent antibacterial performance for a long time, which was convenient for the preparation and storage of the material. C/PVA/SA gel beads could enhance the versatility and portability of antibacterial materials. The antibacterial properties of prepared gel beads against *E. coli*, *S. aureus*, *P. aeruginosa*, and the silver-loaded fish-scale biochar antibacterial mechanisms were tested. Furthermore, the reusability, days of stability, and antibacterial effect of gel beads at different pH were examined. Moreover, the influences of PVA and SA adhesiveness on the gel bead swelling, water loss rate, shrinkage rate, and degradation ability of the gel beads were measured. Overall, this work focused on exploring the antibacterial ability and universality of antibacterial gel beads, which show potential application in the treatment of microbial contamination and environmental protection.

2. Materials and Methods

2.1. Chemicals and Bacteria

All the reagents used in this study were of analytical grade. Polyvinyl alcohol (PVA $\geq$ 98.0%), sodium alginate (SA), calcium chloride ($CaCl_2$ $\geq$ 99.8%), silver nitrate ($AgNO_3$ $\geq$ 99.8%), sodium chloride (NaCl $\geq$ 99.5%), and the trisodium citrate diaqueous mixture ($C_6H_5Na_3O_7 \cdot 2H_2O$ $\geq$ 99.0%) were bought from Runyou Reagents Co., (Changzhou, China). Yeast powder, tryptone, and agar were obtained from Oxoid (Shanghai, China). The waste fish scales were from a local market in Nanjing, China. *E. coli* ATCC 25922,

P. aeruginosa ATCC 9027, and *S. aureus* ATCC 6538 were bought from the Microbiology Institute of Shanghai (China).

2.2. Preparation of C-Ag

The C-Ag preparation is displayed in Figure 1. The treated and dried fish scales were calcined in a muffle furnace (300 °C) for 120 min. Then, 5.0 g of carbonized fish scale powder was added into 100 mL of silver nitrate (0.50 g/L) solution by stirring for 120 min. Trisodium citrate (0.20 g) was added to the above solution to reduce the silver ions and soaked for 1 day, filtered, and dried. Subsequently, the material was placed in a muffle furnace, which was gradually heated to the designed temperature (250 °C) at a heating speed of 10 °C per minute, and maintained at a high temperature for 120 min. Finally, the C-Ag composite was extracted and milled into powder [23].

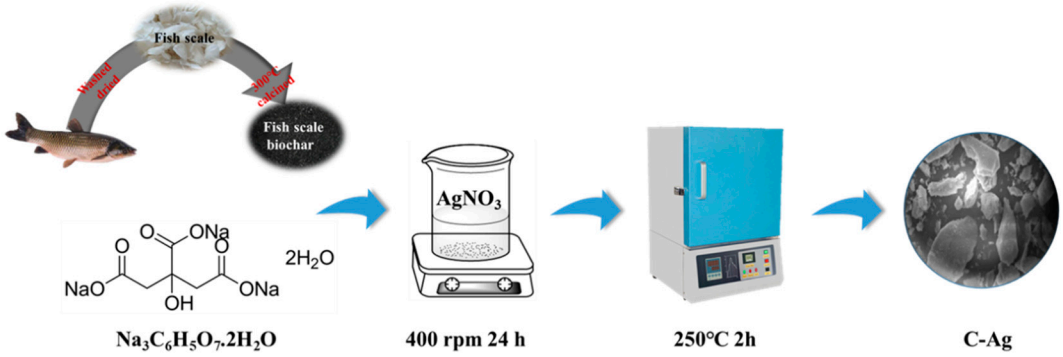

Figure 1. The scheme for preparing C-Ag.

2.3. Preparation of SA/PVA/C–Ag Gel Beads

A 2% SA solution and a 4% PVA solution were prepared, and 2.0 g/L of silver-loaded carbon was added to the 2% SA solution, stirred evenly, sonicated, and left to stand for defoaming. Subsequently, the SA/PVA/C-Ag solution was drawn up into a syringe, and dropped into 45 mL of 10% $CaCl_2$ solution. The mixture was placed in a refrigerator at 4 °C for 12 h, then washed with deionized water many times. Finally, it was dried at 50 °C in a vacuum drying oven to produce the SA/PVA/C-Ag gel beads.

2.4. Characterization of SA/PVA/C–Ag Gel Beads

A Fourier-transform infrared spectrometer (FT-IR) (Nicolet iS50, Thermo Scientific Co., Waltham, MA, USA) in the range of 500–4000 cm^{-1} was utilized to analyze the SA/PVA/C-Ag gel beads.

2.5. Antibacterial Testing

E. coli ATCC 25922, *S. aureus* 6538, and *P. aeruginosa* 9024 were utilized to test the antibacterial ability of the antibacterial materials. All the glassware used in the antibacterial experiments was sterilized by autoclaving (121 °C, 20 min). The antibacterial activity of the materials against the bacteria was determined with plate counts, and the good diffusion method was employed to evaluate the antibacterial effect. The bacterial suspension (100 µL) was coated on an agar LB solid medium, and the hole was 9 mm [24]. An amount of 0.10 g of SA/PVA/C-Ag gel beads was added to the well and incubated at 37 °C for 1 day, and the inhibition of the growth of bacteria around the material was measured [25]. All the experiments were performed in triplicate and then averaged.

The antibacterial rate (AR) was defined as below:

$$\text{Antibacterial rate}(\%) = \frac{A0 - A1}{A0} \times 100$$

where A0 is the number of initial colonies, and A1 is the number of colonies treated with the SA/PVA/C-Ag gel beads.

2.6. The Materials and C-Ag Dosage Optimization of the SA/PVA/C–Ag Gel Beads

The gel beads synthesized with SA and PVA were denoted as S/P. The SA gel bead loading C-Ag was denoted as S/A. Various loadings of C-Ag were fixed on PVA and SA gel beads denoted as S/P/A (A content: 0.2, 0.4, 0.6, 0.8, 1.0, and 1.2%). The inhibition of microbial growth was measured by the good diffusion method to assay the best material combination and C-Ag concentration. To ensure the accuracy of the experiment, three sets of parallel samples were made, and the recorded data were averaged.

2.7. The Dosage and Time Optimization of the SA/PVA/C–Ag Gel Beads

To test the antibacterial effect of the composite at different doses and times, optimization experiments were carried out with *E. coli*, *S. aureus*, and *P. aeruginosa* as the experimental objects. The initial concentration of the bacterial suspension was 10^8 CFU/mL [26]. The dosage of the composites was 0.5, 1.0, 1.5, 2.0, 2.5, and 3 g/L. The antibacterial materials were blended with the bacterial suspensions and incubated in a 37 °C thermostatic container. After 1, 3, 5, 7, and 9 h, 0.10 mL of the suspension was used to test the antibacterial abilities of the antibacterial materials by plate counting. The experiment was repeated three times to ensure the reliability of the experiment.

2.8. Antibacterial Reusability and Stability

The reusability of SA/PVA/C-Ag gel beads is an important factor in practical applications [27]. The antibacterial tests of three kinds of bacteria (*E. coli*, *S. aureus*, and *P. aeruginosa*) were performed separately in water. The SA/PVA/C-Ag gel bead was removed and washed with deionized water for the next cycle of experiments. The composites were repeatedly used 10 times. Then, the gel bead's bacteriostatic performance was evaluated. After ten iterations of antibacterial tests, the antibacterial motive of the gel beads against the three kinds of bacteria was above 90%.

The stability of SA/PVA/C-Ag gel beads is another factor in daily bacteriostasis [11]. A batch of SA/PVA/C-Ag gel beads were prepared and left at room temperature. The antibacterial performance was tested on days 1, 3, 5, 7, 9, 11, 13, and 15. The antibacterial gel beads maintained >99% antibacterial performance during the 15 days of testing. A good antibacterial effect under different pH conditions is indicative of a wide application potential of antibacterial materials [28]. The gel beads were left overnight in a PBS solution at pH 3, 5, 7, 9, and 11 and subsequently removed for an evaluation of antibacterial properties. The antibacterial test results displayed that the gel beads had excellent antibacterial performance in different water environments. All the experiments were performed in triplicate and then averaged.

2.9. Swelling Ratio of SA/PVA/C-Ag Gel Beads

The swelling rate of antibacterial materials used in water is one of the most important indicators of their properties [29]. Ten dry SA/PVA/C-Ag gel bead particles were prepared in advance with different PVA concentrations (2, 4, 6, 8, 10, and 12%) and weighed. The gel beads were placed in deionized water and removed from the water every hour. The surface water was wiped off with filter paper, and then the quality data were measured and recorded.

A good antibacterial effect of antibacterial materials in different pH solutions is also one of the important factors for practical application [30]. Ten SA/PVA (4%)/C-Ag gel beads were dried and weighed. Then, the gel beads were placed in a solution with different pH concentrations, and removed from the water every 60 min; the surface water was wiped off, the mass was measured, and the data were recorded. The above experiment was repeated three times to ensure the reliability of the data.

The expansion ratio (ER) formula was defined as below:

$$\mathrm{ER}(\%) = \frac{\mathrm{M1} - \mathrm{M0}}{\mathrm{M0}} \times 100$$

where M1 is the mass of the pellet at some point, and M0 is the mass of the initial dry pellet.

2.10. Morphological Properties, Water Loss, and Shrinkage of SA/PVA/C-Ag Gel Beads

The gel beads prepared with different materials were dried, and the diameter of the gel beads was measured with a vernier caliper. Then, the microstructure of the four gel beads was observed using a mobile phone camera (HUAWEI P50 PRO, HUAWEI Inc., Shenzhen, China).

Gel beads with different PVA concentrations (2, 4, 6, 8, 10, and 12%) were prepared and left for later use. Five gel beads with different PVA concentrations were taken out and dried. They were put into the oven at 80 °C for 1, 2, 3, 4, 5, 6, 8, 10, 20, and 30 min, and then taken out and weighed, and the mass loss was recorded [31]. The effect of the PVA on the water loss rate of the gel beads was observed. The experiment was repeated three times as the PVA concentration increased and the water loss rate decreased.

The water loss ratio (WLR) formula was as below:

$$\mathrm{WLR}(\%) = \frac{\mathrm{W0} - \mathrm{W1}}{\mathrm{W0}} \times 100$$

where W1 is the mass of the gel beads at some point, and W0 is the mass of the initial gel beads.

Gel solutions with different PVA concentrations were dropped into a $CaCl_2$ solution, and the slice shrinkage rate of the gel beads was determined at 2, 4, 6, 8, 10, 20, and 30 min [32]. Five gel beads with different PVA concentrations were obtained from the $CaCl_2$ solution and washed with distilled water. After surface drying, the long half-axis (r1max) and small half-axis (r1min) of the gel beads were assayed with a digital vernier caliper, and the cross-sectional area (A1s = r1max × r1min) was calculated. The major half-axis (r0max) and minor half-axis (r0min) of the gel beads were assayed after 1 min of gelation, and the cross-sectional area (A0s = r0max × r0min) was measured. In this work, the cross-sectional shrinkage rate of the sample during the gelation process was compared with the cross-sectional area of the sample after 60 s of gelation. The experimental data were recorded, and the experiment was repeated three times.

The section shrinkage rate (SSR) formula was as below:

$$\mathrm{SSR}(\%) = \frac{\mathrm{A0s} - \mathrm{A1s}}{\mathrm{A0s}} = \frac{3.14 \times \mathrm{r0max} \times \mathrm{r0min} - 3.14 \times \mathrm{r1max} \times \mathrm{r1min}}{3.14 \times \mathrm{r0max} \times \mathrm{r0min}} \times 100$$

2.11. Degradation of SA/PVA/C-Ag Gel Beads

The degradation performance of antibacterial materials is an indicator of the environmental protection performance of materials [33]. The prepared SA/PVA/C-Ag gel beads were buried in natural soil without any enzymatic activity, and the relatively mild temperature was maintained at 30 °C and 80% humidity. Samples of the same mass were removed every 5 days, and the gel beads were rinsed with water to remove dirt from the sample. The morphological characteristics of the gel beads were photographed and recorded. After drying, the weight before and after burial was assayed in a constant temperature drying oven as data for the biodegradability assessment. Three sets of parallel samples were made, and the data were recorded and averaged.

The degradation rate (DR) formula was as below:

$$\mathrm{DR}(\%) = \frac{\mathrm{W1} - \mathrm{W2}}{\mathrm{W1}} \times 100$$

where W1 and W2 are the weight of the sample before and after being buried.

3. Result and Discussion

3.1. Characterization of SA/PVA/C-Ag Gel Bead Composite

Fourier-Transform Infrared (FT-IR) Spectrometry Analysis

The FT-IR spectra of the SA gel beads, the SA/C-Ag gel beads, the SA/PVA gel beads, and the SA/PVA/C-Ag gel beads are displayed in Figure 2. The enhanced peak at 3437 cm^{-1} was attributed to the generation of hydrogen bonds between the biochar and the -OH group of the PVA matrix [34]. The peaks at about 2972 cm^{-1} and 1433 cm^{-1} corresponded to the C-H tensile and bending vibrations [26]. The asymmetric and symmetric carboxylate stretched nearly 1631 cm^{-1} and 1388 cm^{-1}, indicating that PVA and SA interact through hydrogen bonds [35]. The characteristic peak at 1599 cm^{-1} belonged to the N-H tensile vibration. The C-C stretching vibration absorption peak was located at 1353 cm^{-1} [22]. The characteristic peaks at 1077 cm^{-1} and 1020 cm^{-1} corresponded to the vibrational frequencies of C-N/O and C-O-C [36]. The absorption peak of the C-H bending vibration existed at 770 cm^{-1}. The absorption peak generated by the rotation of the -OH was located at 615 cm^{-1} [10].

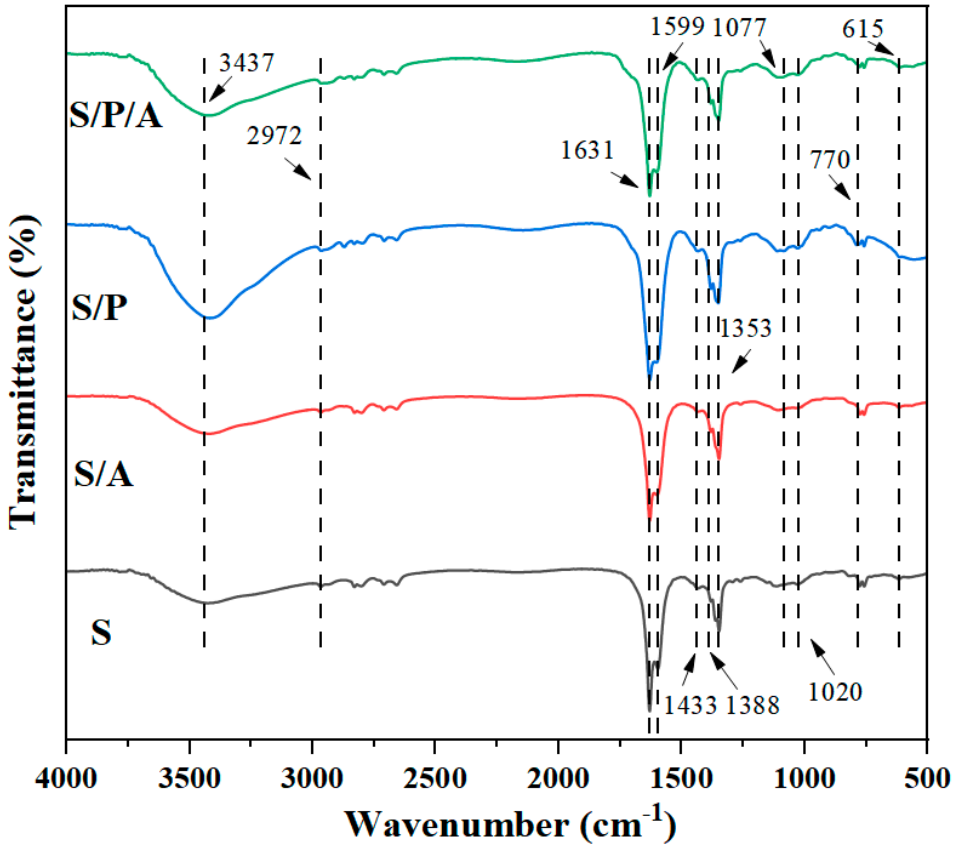

Figure 2. FT-IR spectra of SA gel beads, SA/C-Ag gel beads, SA/PVA gel beads, and SA/PVA/C-Ag gel beads.

3.2. Antibacterial Properties

3.2.1. Effect of the Materials and C-Ag Dosage

The materials used to prepare the gel beads and the loading of antibacterial substances may affect the bacteriostatic effectiveness [37]. Through SEM analysis of C-Ag, silver nanoparticles were successfully prepared and attached to the surface of fish-scale biochar (Figure S1a,b). Figure 3a displays that the gel beads formed by PVA and SA had no antibacterial effect. Tetracycline had the most obvious inhibitory effect on bacteria. The antibacterial effect of the gel beads prepared with the same dose of silver-loaded carbon was obvious by the PVA added. PVA is a water-soluble polymer material that plays the role

of hydrophobic swelling [38]. Silver ions are released through the PVA adhesive structure to inhibit bacteria [39]. With the increase of silver-loaded carbon, the gel beads liberated more Ag^+, and the antibacterial effect reached its peak at the dose of 1.0 g/L (Figure 3b). An analysis of variance (ANOVA) was used to assess and identify the significant factors (the effect of silver ion concentration on bacteriostasis). The SA/PVA/C-Ag gel beads loaded with silver–carbon played a bacteriostatic effect, and the PVA provided a release channel for the silver ions, forming a synergistic bacteriostatic effect.

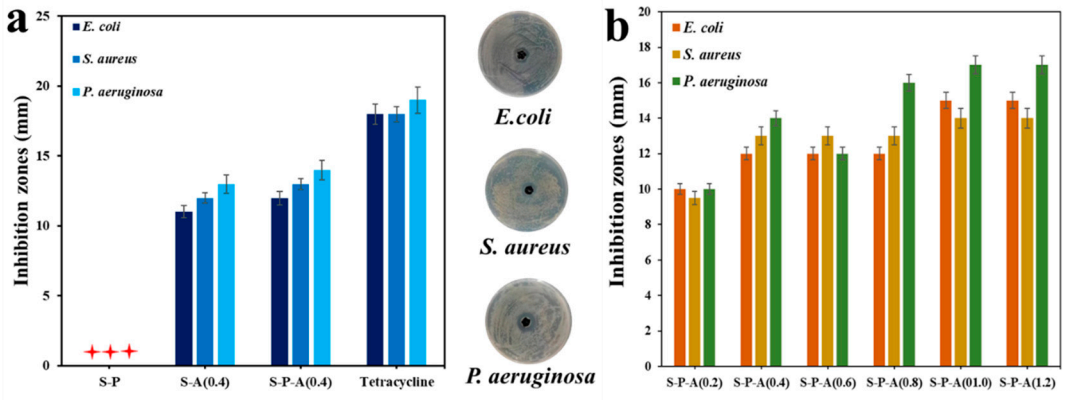

Figure 3. Antibacterial effects of gel beads prepared from different materials and antibacterial effects of tetracycline (**a**). Antibacterial effects of gel beads containing different dosages of silver-loaded carbon (C-Ag: 0.2, 0.4, 0.6, 0.8, 1.0, and 1.2 g/L) (**b**). +++ no antibacterial effect.

3.2.2. The Dosage and Time Optimization of the SA/PVA/C–Ag Gel Beads

The dosage and action time of antibacterial materials are important indexes to evaluate the practical application of antibacterial materials. With an increase in material dose and release time, the antibacterial effect could be enhanced [40]. With the increase in SA/PVA/C-Ag gel bead dosage and antibacterial time, the antibacterial effect had a significant change (Figure 4). The SA/PVA/C-Ag gel beads had an obvious inhibitory influence on the growth of *E. coli* (Figure 4a). At the time points of 1 h and 3 h, the effects of increasing the dose of SA/PVA/C-Ag gel beads were greatly improved. At 9 h, the inhibition rate reached over 95%. The increase in gel bead dosage did not promote the antibacterial effect. Many studies have used *E. coli* as the standard strain [41]. The antibacterial effect of 0.80 g/L antibacterial materials reached 90% within 7 h [26]. The gel bead dosage of 0.50 g/L could achieve above a 90% inhibition rate within 7 h. And the silver-loaded carbon content of the gel beads was lower, which played the role of decreasing the cost and maximizing the effect.

S. aureus is a common foodborne pathogenic microorganism of Gram-positive bacteria [42]. The inhibition rate of *S. aureus* was 95% in some bacterial materials targeted at inhibiting *S. aureus* [43]. In this work, the gel bead dosage was 3 g/L, the inhibition time was 9 h, and the inhibition rate was over 95% (Figure 4b). The bacteriostatic effect was improved greatly with the increase in bacteriostatic time when the gel bead dose was low. According to the antibacterial results, the SA/PVA/C-Ag gel beads had a good inhibitory effect on *S. aureus*.

In the antibacterial tests, the SA/PVA/C-Ag gel beads had a clear inhibitory effect on *P. aeruginosa*. *P. aeruginosa* is one of the most common bacteria in the world [44]. It has strong resistance and good adaptability to natural antibacterial materials [45]. In the bacteriostatic experiment over 60 min, the bacteriostatic rate was over 90% when the gel bead dose was 0.50 g/L. With the increase in the dosage of antibacterial materials, the inhibition rate was raised (Figure 4c). The bacteriostatic time reached more than 180 min, and the bacteriostatic rate of the minimum dose of bacteriostatic material reached >99%. The inhibitory effect of the material on bacteria no longer increased obviously with the increase in dosage.

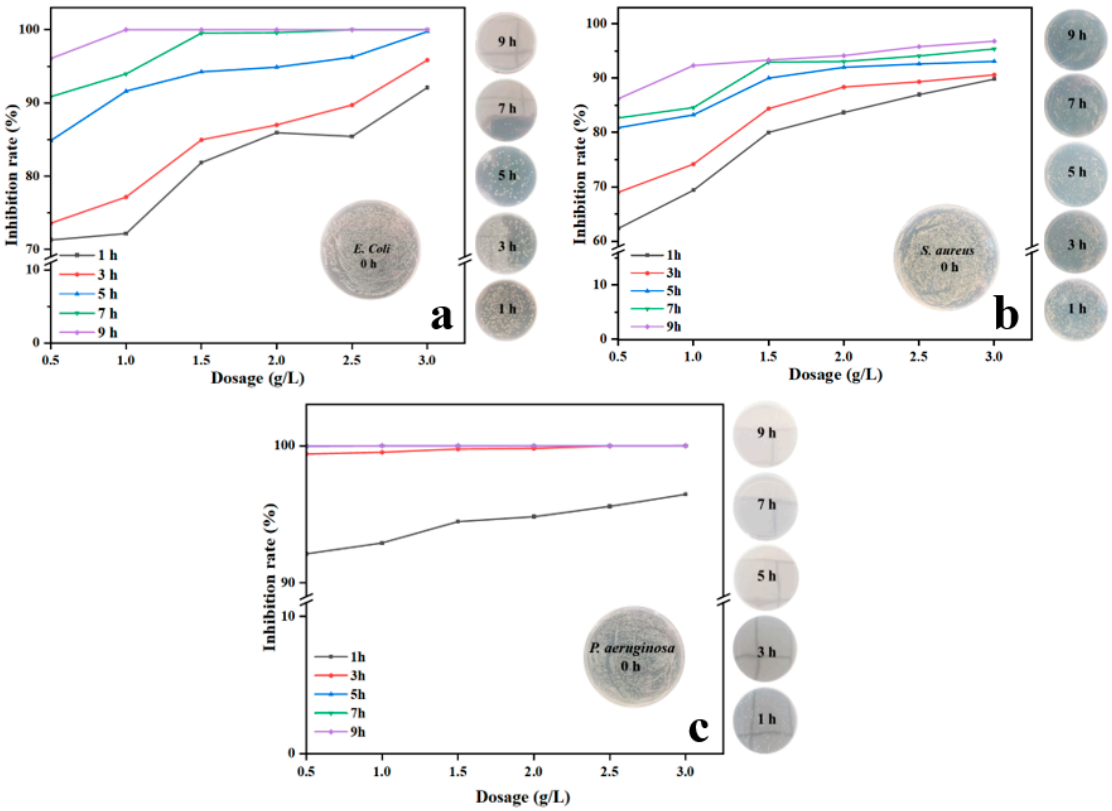

Figure 4. Antibacterial rate images of the SA/PVA/C–Ag gel beads on bacteria *E. coli* (**a**), *S. aureus* (**b**), and *P. aeruginosa* (**c**) at different material dosages and release times.

The antibacterial test results displayed that the SA/PVA/C-Ag gel beads had a clear inhibitory effect on both Gram-negative and Gram-positive bacteria. The results indicated that the gel beads had strong bactericidal performance in water with a small dosage. The composite material had great potential in water applications.

3.2.3. Antibacterial Reusability and Stability of SA/PVA/C–Ag Gel Beads

The performance stability and reusability of antibacterial materials are key elements in practical antibacterial applications [22]. A long storage time of antibacterial materials and a high inhibition rate after multiple antibacterial tests will reduce the application cost. Figure 5 indicates that the SA/PVA/C-Ag gel beads had stable antibacterial performance and good reusability in different environments. Within 15 days of the gel bead preparation, the inhibition effect on *E. coli* and *P. aeruginosa* reached 100%. The effect against *S. aureus* decreased slightly, with an inhibition rate of >98.5% (Figure 5a). In some stability tests of bacteriostatic materials, when the completion time was 15 days, the bacteriostatic rate declined to 90% [26]. As revealed in Figure 5b, from the repeated inhibition test of *E. coli* and *P. aeruginosa*, the gel beads had an obvious inhibition effect on bacterial growth, with an inhibition rate of 97%. When the second antibacterial test in water was over, the antibacterial effect of the gel bead composite material began to drop slightly. When the experiment was completed for the 10^{th} time, the inhibitory effect of the bacteriostatic materials on bacterial growth was weakened clearly, and the bacteriostatic rate reached about 90%. Natural antibacterial materials were generally not durable, and the antibacterial effect would be weakened after repeating the test 5 times [46].

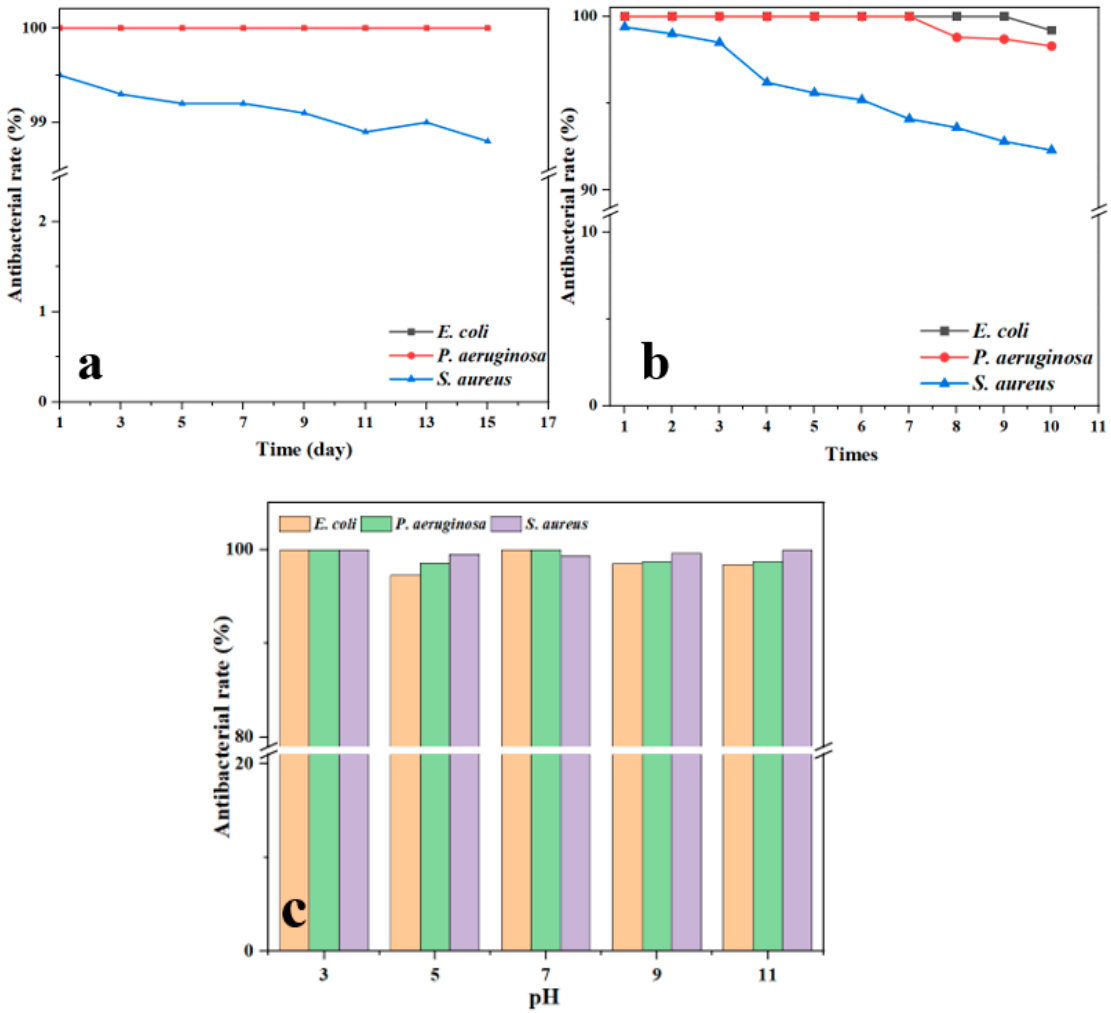

Figure 5. Antibacterial effect images of SA/PVA/C-Ag gel beads prepared on different days (**a**), repetitive antibacterial properties (**b**), and different pH solutions (**c**).

When the gel beads were left in different pH solutions (pH: 3, 5, 7, 9, and 11) overnight, the antibacterial effect didn't change significantly (Figure 5c). Maintaining efficient antibacterial performance in different media environments is an important criterion for the application of antibacterial materials [47]. The results of bacterial inhibition indicated that the antibacterial substances in the gel beads did not change greatly in acidic and alkaline media and maintained high antibacterial performance.

The above results suggest that gel beads have strong stability and good reusability. According to the researchers report on PVA/SA gel, the high hydrophilic property of PVA increased the hydrophobic property of gel beads [17]. When the silver-loaded carbon was loaded inside the SA gel beads, AgNPs were released through the hydrophobic structure constructed by the PVA. PVA shrinkage during storage would lock AgNPs firmly into the gel beads. The gel beads of SA/C-Ag with PVA as a reinforcer assisted the liberation of Ag^+ through the adhesive structure of the PVA and SA to improve the antibacterial effect.

3.3. Physical Properties

3.3.1. Swelling Ratio of SA/PVA/C-Ag Gel Beads

The swelling rate of antibacterial material in water is one of the key indexes of its performance [48]. The swelling rate of materials provides an important reference point in daily practice. Within a set period, the swelling rate of the material was raised with the increase in the soaking time (Figure 6a). When the PVA content was 2%, 4%, 6%, and 8%, the gel bead swelling reached equilibrium at 7 h. The swelling of the gel beads with 6%

and 8% PVA content started to drop slightly after a few hours when the swelling reached equilibrium. Due to the high hydrophilicity of PVA, the gel beads began to dissolve. When the PVA content of the gel beads was 10% and 12%, the swelling rate began to drop after 1 h of swelling. Due to the high PVA content, the gel beads dissolved faster. Figure 5a indicated that the highest swelling rate was 350% when the PVA content of gel beads was 4% and 6%. Because the gel beads would dissolve when the PVA load was 6%, the gel beads with 4% of PVA had the best swelling performance. The additional load of PVA could regulate the hydrophobic structure of the gel beads and improve the swelling performance of gel beads under the suitable PVA load. The swelling property of the gel class was between 300% and 400% [22].

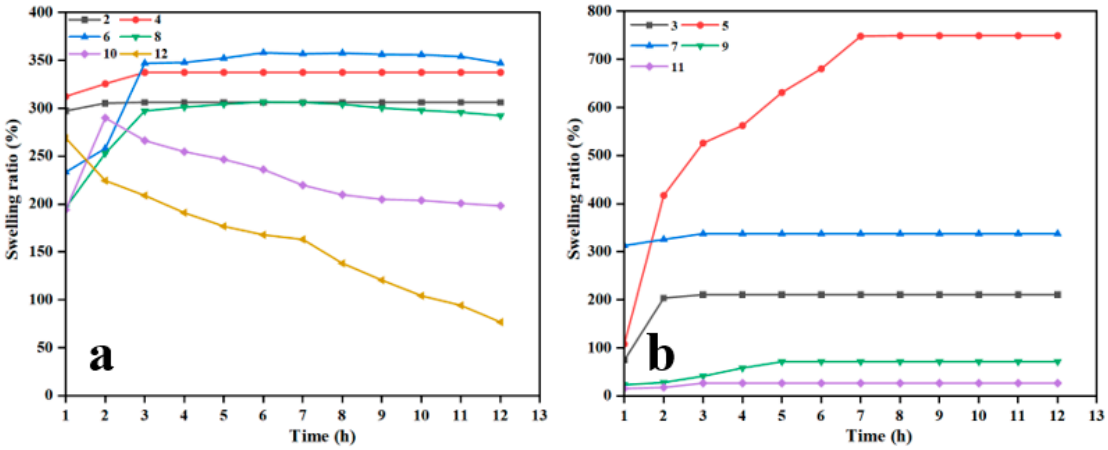

Figure 6. Swelling effect images of different PVA dosages (**a**) and different pH solutions (**b**) in 12 h.

The PVA content of the gel beads in the pH swelling experiment was 4% (Figure 6b). The prepared gel beads were placed into different pH of media for 12 h. In the pH 3.0 medium, the swelling rate was 200%. Calcium alginate (CA) shell formed when a sodium alginate solution met a $CaCl_2$ solution, which could protect the acid solution from rupture [49]. In the pH 5.0 medium, the swelling rate of the gel beads obviously increased to 749%. The hydrophobic structure of PVA in gel beads greatly increased the swelling rate of gel beads in solution [50]. When the pH was greater than pH 7.0, the swelling rate was less than 100%. The PVA was difficult to dissolve in an alkaline solution [51], and the shrinkage and swelling rate of the hydrophobic structure constructed by the PVA dropped in the alkaline solution. The swelling test results displayed that the swelling ability of gel beads was greatly enhanced in a neutral acidic solution.

3.3.2. Morphological Properties, Shrinkage, and Water Loss of SA/PVA/C-Ag Gel Beads

As illustrated in Figure 7, the SA gel beads were transparent (a), and the SA gel beads were black when loaded with silver–carbon (b). The gel beads synthesized by SA and PVA were cloudy and opaque in color (c), and dark gray when silver-loaded carbon was added (d). In this study, the simple drop method was utilized to prepare the emulsion gel beads. The gel solution was pushed out of the pipette to form a droplet at the tip, which was then dropped into the $CaCl_2$ solution. After PVA was added to the gel solution, the viscosity of the gel beads became larger.

In the water-loss test experiment, with the increase in time in the oven, the Ca^{2+} infused from the surface of the gel beads to the interior, and the interchain interaction between the stretched segments of the alginate monomer and Ca^{2+} occurred. The connection between these stretched segments could force water to flow out, resulting in an increased water loss in the gelation of the gel beads [52]. Figure 8a reveals the effect of PVA dosage on the water loss of the gel beads. With the increase in PVA loading, the water-loss rate of the gel beads dropped. When the PVA content in the gel beads was 12%, the moisture content was close to 40% after drying in the oven at 80 °C for 30 min. Silver-loaded carbon

was added to SA and PVA gel beads, and the gel beads loaded with silver-loaded carbon had better water retention ability at the same PVA concentration. Due to the hydrophilic and film-forming properties of PVA [17], the gel beads formed by the adhesion of sodium alginate and PVA had a complex pore structure that could lock in more water to prevent water loss [11]. The addition of silver-loaded carbon made the internal structure of the gel beads more complex, and the water loss rate was lower. Some studies have shown that biochar has a certain adsorption capacity and a certain water-locking property [26]. The PVA and silver-loaded carbon increased the adsorption and water-locking properties of the gel beads, which contributed to a new idea for gel bead materials.

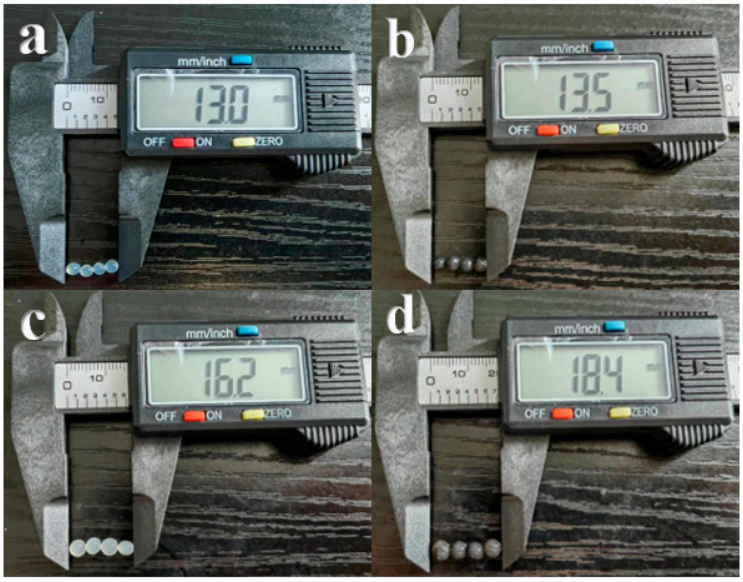

Figure 7. Visual aspects of gel beads prepared from different materials. SA gel beads (**a**). SA and C-Ag gel beads (**b**). SA and PVA gel beads (**c**). SA, PVA, and C-Ag gel beads (**d**).

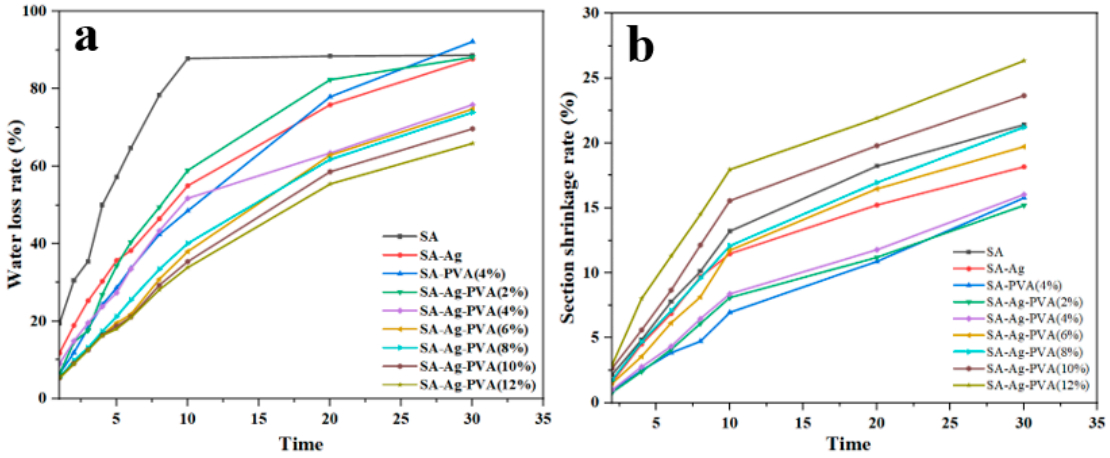

Figure 8. Water-loss (**a**) and shrinkage (**b**) images of gel beads with different PVA contents.

Over the process of the gel bead formation, the gel beads shrink as time increases and finally reach equilibrium [49]. Figure 8b illustrates that all the samples decreased in size during gelation, and, to compare their shrinkage during gelation, the cross-sectional shrinkage was calculated. The shrinkage of the samples during gelation was probably due to dehydration and structural collapse [53]. As can be seen in the shrinkage curve, increasing the content of PVA increased the shrinkage, and increasing the gelation duration had an obvious influence on the shrinkage in the gelation process. The shrinkage rate of 12% PVA was 26.3%, and the supplementation of a certain content of PVA was helpful

to the shrinkage of the gel beads. The results of the morphological properties, shrinkage, and water loss indicate that PVA greatly enhanced the mechanical properties of the gel beads, and the silver-loaded biochar enhanced the physical properties of the gel beads to a certain extent.

3.3.3. The Degradation of SA/PVA/C–Ag Gel Beads

In some studies, degradation property is an important criterion for materials [54]. The degradation properties of materials have been paid more and more attention by researchers [55]. The gel beads containing PVA had the best degradation performance, and the adhesive structure constructed by the PVA and SA was conducive to the degradation of the gel beads. However, the biochar was difficult to degrade, which hindered the degradation of the gel beads (Figure 9). The degradation results in this study were close to some of the composite gel results, and had no damage to the environment in the treatment of bacteriosis [56]. The beads are a bacteriostatic material with market potential and environmental protection.

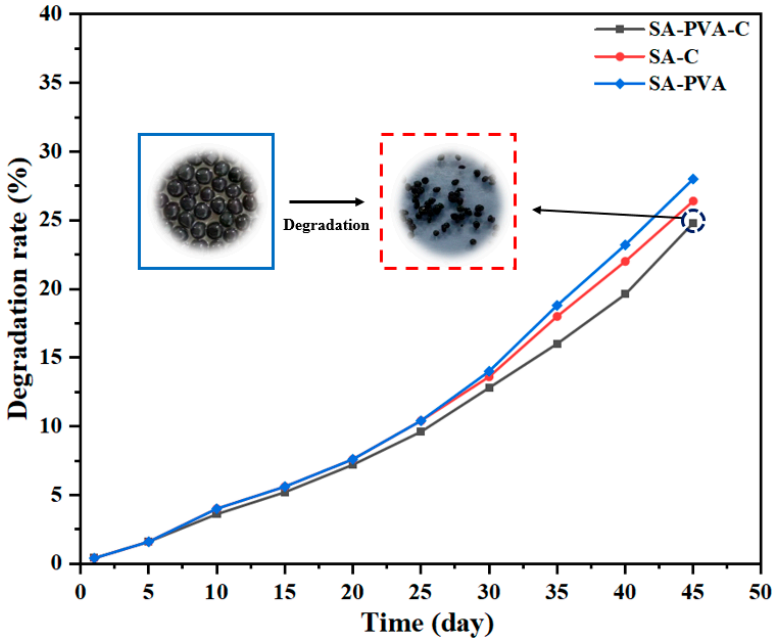

Figure 9. The degradation curve images of SA/PVA/C-Ag gel beads.

3.4. The Mechanism of Bacterial Inhibition by SA/PVA/C-Ag Gel Beads

Biochar materials have been widely used as carriers of nano-metal ions in antibacterial and catalysis processes [4,57–63]. PVA is a kind of network polymer with a cross-network structure. In the bacteriostasis process of SA/PVA/C-Ag gel, the network hydrophobic structure provided by the PVA and SA provides a carrier for dispersing fish-scale silver-loaded carbon (C-Ag). The porous structure and large specific surface area of fish scales after carbonization also provided suitable conditions for loading silver [10]. Due to the extensive and long-lasting bactericidal ability of silver [40], the fish-scale biochar loaded with silver had a strong bactericidal effect. When the gel bead was immersed in water, the internal network hydrophobic structure made the gel bead expand [50], so that the antibacterial material was able to fully contact the water environment. The silver nanoparticles on the C-Ag composite were liberated into the water through the network hydrophobic structure to result in a continuous sterilizing effect.

After AgNPs come in contact with bacteria, the AgNPs can pass through the cell membrane and enter the cytoplasm, due to the change in charge inside and outside the cell, thus destroying the internal structure of the cell [64]. AgNPs also damage the cell membrane, causing material inside the cell to leak out, leading to the death of the bacteria [65].

The interaction of AgNPs with mitochondrial respiratory enzymes after entering the cell wall would lead to the proliferation of reactive oxygen species [66], ultimately causing the disruption of ion transport channels. As a result, many cellular metabolic processes (such as DNA synthesis, protein and ribosome destruction, and enzyme synthesis) are disrupted [67,68], ultimately leading to bacterial inactivation. The large contact area of gel beads provides a platform for the interaction of bacteria and bacteriostatic agents [69–74], which further promotes microbial destruction [66,67]. In this work, the bonding network structure of PVA and SA was constructed (Figure 10), and the silver-biochar loaded on fish scales was fully loaded in the network structure to give full play to the antibacterial effect of the antibacterial materials. The production cost of the experimental material pair was reduced, and the continuous antibacterial performance of the antibacterial material was improved, which has a good application prospect in water treatment application materials.

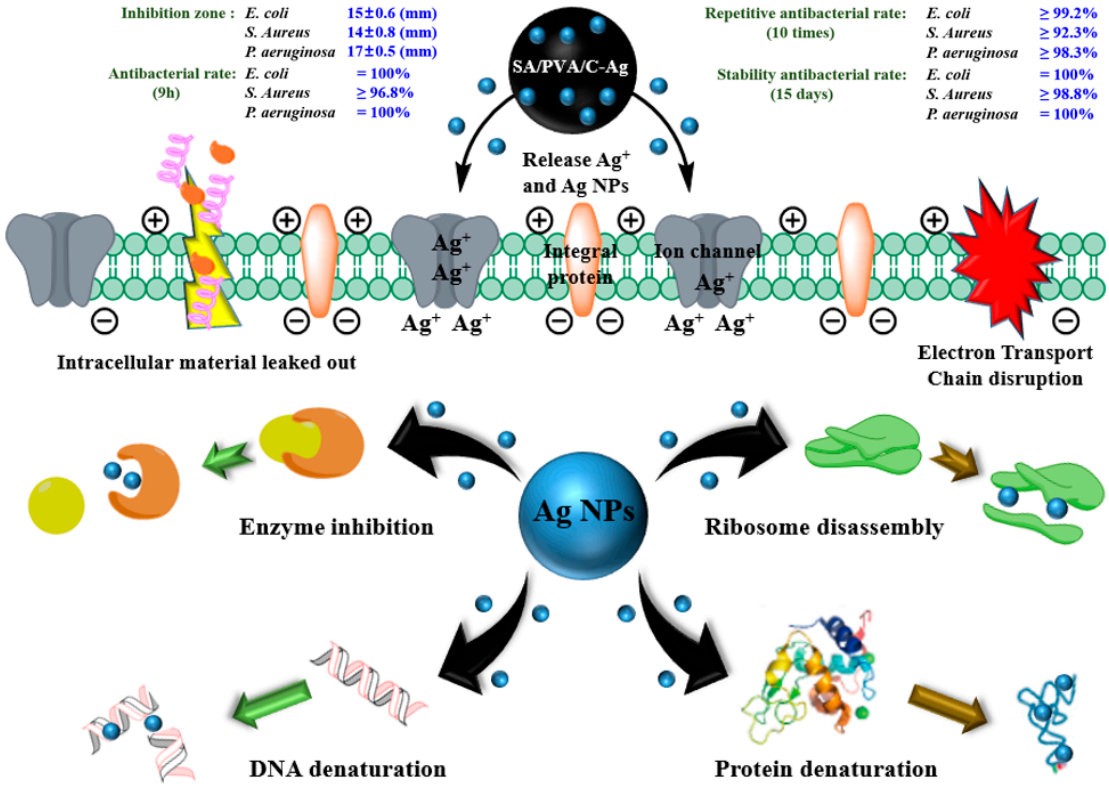

Figure 10. Antibacterial mechanism of SA/PVA/C-Ag gel beads.

4. Conclusions

As society and the economy develop, human activities will continue to discharge industrial and agricultural pollutants into water bodies, and water microbial pollution is becoming increasingly serious. Accordingly, the development of a long-term, efficient, low-cost, eco-friendly biochar-based composite material with excellent antibacterial properties has gained much attention. Fish scales are easy to obtain, and the silver-carrying biochar-polyvinyl alcohol-alginate gel beads (C/PVA/SA) can be easily prepared. The fish-scale biochar was loaded with Ag^+ by high-temperature reduction. SA/PVA/C-Ag gel beads with complex hydrophobic structures were synthesized. FTIR characterization confirmed the successful preparation of the material. The antibacterial test results indicated that a large number of silver ions loaded on the fish-scale silver-biochar provided a good antibacterial effect in the SA/PVA/C-Ag gel beads. A hydrophobic structure was constructed in the gel beads through the adhesive interaction of PVA and sodium alginate, which improved the release of silver ions from the silver-loaded fish-scale biochar. It had an obvious inhibitory effect on *E. coli*, *S. aureus*, and *P. aeruginosa*. In the physical properties test, the SA/PVA/C-

Ag gel beads had high swelling properties. The swelling rate was increased in an acidic solution. PVA provided stability for the gel beads in alkaline solutions. The addition of PVA reduced the water loss rate and increased the shrinkage rate of gel beads so that the gel beads had good physical properties. The porous structure of fish-scale biochar also reduces the water-loss rate. The hydrophobic structure of PVA and sodium alginate also improved the degradation rate of the gel bead pairs. Overall, this prepared material is a new type of antibacterial gel bead, which has good antibacterial properties, good performance stability, and excellent recyclability and portability. In addition, the good degradation performance of the C/PVA/SA was in line with the concept of environmental protection. Consequently, these newly prepared C/PVA/SA gels have high potential application for the treatment of sewage in a high-efficiency reactor on a large scale in the future.

Supplementary Materials: The following supporting information can be downloaded at: https://www.mdpi.com/article/10.3390/pr11082330/s1, Figure S1. SEM images of C-Ag 10,000 magnification (a,b).

Author Contributions: Conceptualization, methodology and writing—original draft, L.X. and Z.Z.; data curation, software, supervision, review and revising manuscript, Y.H. All authors have read and agreed to the published version of the manuscript.

Funding: This research received no external funding.

Institutional Review Board Statement: Not applicable.

Informed Consent Statement: Not applicable.

Data Availability Statement: Not applicable.

Acknowledgments: The authors thank the Analysis and Testing Center (Changzhou University) for the analysis of samples with FT-IR, SEM, XRD, etc.

Conflicts of Interest: The authors declare no conflict of interest.

References

1. He, Q.; Zhang, H.; Ma, M.; He, Y.; Jia, J.; Hu, Q.; Gong, Y. Critical assessment of protozoa contamination and control measures in mass culture of the diatom *Phaeodactylum tricornutum*. *Bioresour. Technol.* **2022**, *359*, 127460. [CrossRef]
2. Yang, W.; Cai, C.; Guo, Y.; Wu, H.; Guo, Y.; Dai, X. Diversity and fate of human pathogenic bacteria, fungi, protozoa, and viruses in full-scale sludge treatment plants. *J. Clean. Prod.* **2022**, *380*, 134990. [CrossRef]
3. Rodwihok, C.; Suwannakeaw, M.; Charoensri, K.; Wongratanaphisan, D.; Woo, S.W.; Kim, H.S. Alkali/zinc-activated fly ash nanocomposites for dye removal and antibacterial applications. *Bioresour. Technol.* **2021**, *331*, 125060. [CrossRef]
4. Tomczyk, A.; Sokołowska, Z.; Boguta, P. Biomass type effect on biochar surface characteristic and adsorption capacity relative to silver and copper. *Fuel* **2020**, *78*, 118168. [CrossRef]
5. Kiehbadroudinezhad, M.; Merabet, A.; Hosseinzadeh-Bandbafha, H. A life cycle assessment perspective on biodiesel production from fish wastes for green microgrids in a circular bioeconomy. *Bioresour. Technol. Rep.* **2023**, *21*, 101303. [CrossRef]
6. Chowdhury, P.; Viraraghavan, T.; Srinivasan, A. Biological treatment processes for fish processing wastewater—A review. *Bioresour. Technol.* **2010**, *101*, 439–449. [CrossRef] [PubMed]
7. Goel, N.; Ahmad, R.; Singh, R.; Sood, S.; Khare, S.K. Biologically synthesized silver nanoparticles by *Streptomyces* sp. EMB24 extracts used against the drug-resistant bacteria. *Bioresour. Technol. Rep.* **2021**, *15*, 100753. [CrossRef]
8. Mobaraki, F.; Momeni, M.; Jahromi, M.; Kasmaie, F.M.; Barghbani, M.; Yazdi, M.E.T.; Meshkat, Z.; Shandiz, F.H.; Hosseini, S.M. Apoptotic, antioxidant and cytotoxic properties of synthesized AgNPs using green tea against human. *Process Biochem.* **2022**, *119*, 106–118. [CrossRef]
9. Ashra, N.; Ahmad, F.; Lu, Y.; Yin, D.C. Bacterial extracellular protein interacts with silver ions to produce protein-encapsulated bactericidal AgNPs. *Process Biochem.* **2022**, *106*, 120–129. [CrossRef]
10. Xia, D.; Liu, Y.; Cheng, X.; Gu, P.; Chen, Q.; Zhang, Z. Temperature-tuned fish-scale biochar with two-dimensional homogeneous porous structure: A promising uranium extractant. *Appl. Surf. Sci.* **2022**, *591*, 153136. [CrossRef]
11. Lin, D.; Kelly, A.L.; Maidannyk, V.; Miao, S. Effect of concentrations of alginate, soy protein isolate and sunflower oil on water loss, shrinkage, elastic and structural properties of alginate-based emulsion gel beads during gelation. *Food Hydrocoll.* **2020**, *108*, 105998. [CrossRef]
12. Pal, A.; Khanum, F. Covalent immobilization of xylanase on glutaraldehyde activated alginate beads using response surface methodology: Characterization of immobilized enzyme. *Process Biochem.* **2011**, *46*, 1315–1322. [CrossRef]

13. Bu, X.; Guan, M.; Dai, L.; Ji, N.; Qin, Y.; Xu, X.; Xiong, L.; Shi, R.; Sun, Q. Fabrication of starch-based emulsion gel beads by an inverse gelation technique for loading proanthocyanidin and curcumin. *Food Hydrocoll.* **2023**, *137*, 1083366. [CrossRef]
14. Ji, Y.; Wang, Y.T. Se(VI) reduction by continuous-flow reactors packed with *Shigella fergusonii* strain TB42616 immobilized by Ca^{2+}-alginate gel beads. *Process Biochem.* **2020**, *91*, 46–56. [CrossRef]
15. Lin, D.; Kelly, A.L.; Miao, S. The impact of pH on mechanical properties, storage stability and digestion of alginate-based and soy protein isolate-stabilized emulsion gel beads with encapsulated lycopene. *Food Chem.* **2022**, *372*, 131262. [CrossRef]
16. Jiang, Z.; Zheng, Z.; Wu, J.; Li, X.; Yu, H.; Shen, J. Synthesis, characterization and performance of microorganism-embedded biocomposites of LDH-modified PVA/SA hydrogel beads for enhanced biological nitrogen removal process. *Process Biochem.* **2022**, *121*, 542–552. [CrossRef]
17. Wang, J.; Liang, J.; Sun, L.; Li, G.; Temmink, H.; Rijnaarts, H.H.M. Granule-based immobilization and activity enhancement of anammox biomass via PVA/CS and PVA/CS/Fe gel beads. *Bioresour. Technol.* **2020**, *309*, 123448. [CrossRef]
18. Jeong, D.; Jang, A. Mitigation of self-shading effect in embedded optical fiber in Chlorella sorokiniana immobilized polyvinyl alcohol gel beads. *Chemosphere* **2021**, *283*, 131195. [CrossRef]
19. Wang, Y.; Su, J.; Ali, A.; Chang, Q.; Bai, Y.; Gao, Z. Enhanced nitrate; manganese, and phenol removal by polyvinyl alcohol/sodium alginate with biochar gel beads immobilized bioreactor: Performance, mechanism, and bacterial diversity. *Bioresour. Technol.* **2022**, *348*, 126818. [CrossRef] [PubMed]
20. Uysal, U.; Hamamcı, H. Succinic acid production from cheese whey via fermentation by using alginate immobilized *Actinobacillus succinogenes*. *Bioresour. Technol. Rep.* **2021**, *16*, 100829. [CrossRef]
21. Hazrati, R.; Davaran, S.; Omidi, Y. Bioactive functional scaffolds for stem cells delivery in wound healing and skin regeneration. *React. Funct. Polym.* **2022**, *174*, 105233. [CrossRef]
22. Zhao, H.; Li, X.; Zhang, L.; Hu, Z.; Zhong, L.; Xue, J. Preparation and bacteriostatic research of porous polyvinyl alcohol/biochar/nanosilver polymer gel for drinking water treatment. *Sci. Rep.* **2021**, *11*, 12205. [CrossRef] [PubMed]
23. Zhang, Z.; He, Y. Synthesis and Characteristics of a Fish Scale-Based Biochar–Nanosilver Antibacterial Material. *Processes* **2023**, *11*, 111992. [CrossRef]
24. Zhang, L.; Zheng, S.; Hu, Z.; Zhong, L.; Wang, Y.; Zhang, X.; Xue, J. Preparation of polyvinyl alcohol/bacterial-cellulose-coated biochar–nanosilver antibacterial composite membranes. *Appl. Sci.* **2020**, *10*, 752. [CrossRef]
25. Wu, J.; Zhang, G.; Liu, J.; Gao, H.; Song, C.; Du, H.; Zhang, L.; Gong, Z.; LÜ, Y. Synthesis characteristics, and antibacterial activity of a rare-earth samarium/silver/titanium dioxide inorganic nanomaterials. *J. Rare Earths* **2014**, *32*, 727–732. [CrossRef]
26. Hu, Z.; Zhang, L.; Zhong, L.; Zhou, Y.; Xue, J.; Li, Y. Preparation of an antibacterial chitosan-coated biochar-nanosilver composite for drinking water purification. *Carbohydr. Polym.* **2019**, *219*, 290–297. [CrossRef]
27. Zhang, L.; Bai, X.; Tian, H.; Zhong, L.; Ma, C.; Zhou, Y.; Chen, S.; Li, D. Synthesis of antibacterial film CTS/PVP/TiO_2/Ag for drinking water system. *Carbohydr. Polym.* **2012**, *89*, 1060–1066. [CrossRef]
28. Afshari, M.J.; Sabzi, M.; Jiang, L.; Behshad, Y.; Zanjanijam, A.R.; Mahdavinia, G.R.; Ahmadi, M. Incorporation of dynamic boronate links and Ag nanoparticles into PVA hydrogels for pH-Regulated and prolonged release of methotrexate. *J. Drug Deliv. Sci. Technol.* **2021**, *63*, 102502. [CrossRef]
29. Fuhrmann, P.L.; Powell, J.; Rousseau, D. Structure and rheology of oil-continuous capillary suspensions containing water-swellable cellulose beads and fibres. *Food Hydrocoll.* **2023**, *139*, 108503. [CrossRef]
30. Zeng, H.; Sun, S.; Xu, K.; Zhao, W.; Hao, R.; Zhang, J.; Li, D. Iron-loaded magnetic alginate-chitosan double-gel interpenetrated porous beads for phosphate removal from water: Preparation, adsorption behavior and pH stability. *React. Funct. Polym.* **2022**, *177*, 105328. [CrossRef]
31. Min, C.; Zhang, C.; Cao, Y.; Li, H.; Pu, H.; Huang, J.; Xiong, Y.L. Rheological; textural, and water-immobilizing properties of mung bean starch and flaxseed protein composite gels as potential dysphagia food: The effect of *Astragalus* polysaccharide. *Int. J. Biol. Macromol.* **2023**, *239*, 124236. [CrossRef]
32. Sun, G.; Cheng, L.; Tong, M.; Chen, L.; Luo, J.; Liu, R. Shrinkage stress of thermal cured epoxy resin reduced by addition of functional hollow microspheres. *Prog. Org. Coat.* **2023**, *178*, 107446. [CrossRef]
33. Latif, A.; Maqbool, A.; Sun, K.; Si, Y. Immobilization of Trametes Versicolor laccase on Cu-alginate beads for biocatalytic degradation of bisphenol A in water: Optimized immobilization, degradation and toxicity assessment. *J. Environ. Chem. Eng.* **2022**, *10*, 107089. [CrossRef]
34. Xiang, X.; Yi, X.; Zheng, W.; Li, Y.; Zhang, C.; Wang, X.; Chen, Z.; Huang, M.; Ying, G.G. Enhanced biodegradation of thiamethoxam with a novel polyvinyl alcohol (PVA)/sodium alginate (SA)/biochar immobilized *Chryseobacterium* sp. H5. *J. Hazard. Mater.* **2023**, *443*, 130247. [CrossRef] [PubMed]
35. Ionita, M.; Pandele, M.A.; Iovu, H. Sodium alginate/graphene oxide composite films with enhanced thermal and mechanical properties. *Carbohydr. Polym.* **2013**, *94*, 339–344. [CrossRef] [PubMed]
36. Kuila, S.B.; Ray, S.K. Dehydration of dioxane by pervaporation using filled blend membranes of polyvinyl alcohol and sodium alginate. *Carbohydr. Polym.* **2014**, *101*, 1154–1165. [CrossRef]
37. Anusuya, N.; Pragathiswaran, C.; Mary, J.V. A potential catalyst-TiO_2/ZnO based chitosan gel beads for the reduction of nitro-aromatic compounds aggregated sodium borohydride and their antimicrobial activity. *J. Mol. Struct.* **2021**, *1236*, 130197. [CrossRef]

38. Wang, J.; Liang, J.; Sun, L.; Shen, J.; He, Z. Enhancing anammox resistance to low operating temperatures with the use of PVA gel beads. *Sci. Total Environ.* **2021**, *774*, 144826. [CrossRef]
39. Ingle, J.; Patel, U.D. Electrochemical reduction of nitrate in the presence of silver-coated polyvinyl alcohol beads as a spatially suspended catalyst. *J. Water Process Eng.* **2022**, *49*, 103082. [CrossRef]
40. Abbaszadegan, A.; Ghahramani, Y.; Gholami, A.; Hemmateenejad, B.; Dorostkar, S.; Nabavizadeh, M.; Sharghi, H. The effect of charge at the surface of silver nanoparticles on antimicrobial activity against Gram-Positive and Gram-Negative bacteria: A preliminary study. *J. Nanomater.* **2015**, *2015*, 720654. [CrossRef]
41. Zhang, J.; Su, P.; Xu, T.; Yuan, L.; Qiao, M.; Yang, B.; Zhao, X. Comprehensive study on the role of reactive oxygen species and active chlorine species on the inactivation and subcellular damage of *E. coli* in electrochemical disinfection. *Sep. Purif. Technol.* **2023**, *304*, 122408. [CrossRef]
42. Saha, S.; Malik, M.M.; Qureshi, M.S. Study of synergistic effects of antibiotics and triangular shaped silver nanoparticles, synthesized using UV-light irradiation, on *S. Aureus* and *P. Aeruginosa*. *Mater. Today Proc.* **2019**, *18*, 920–927. [CrossRef]
43. Huang, J.-F.; Shi, Q.-S.; Feng, J.; Chen, M.-J.; Li, W.-R.; Li, L.-Q. Facile pyrolysis preparation of rosin-derived biochar for supporting silver nanoparticles with antibacterial activity. *Compos. Sci. Technol.* **2017**, *145*, 89–95. [CrossRef]
44. Troïa, T.; Siad, J.; Di Giorgio, C.; Brunel, J.M. Design and synthesis of new polyamine quinoline antibiotic enhancers to fight resistant gram-negative *P. aeruginosa* bacteria. *Eur. J. Med. Chem. Rep.* **2022**, *5*, 100054. [CrossRef]
45. Masilan, K.; Neethiselvan, N.; Shakila, R.J.; Muralidharan, N.; Karthy, A.; Ravikumar, T.; Parthiban, F. Investigation on the coacervation of fish scale gelatin hydrogel with seafood waste hydrolysates for the development of artificial fish bait: Physico-chemical, thermodynamic, and morpho-structural properties. *J. Indian Chem. Soc.* **2022**, *99*, 100783. [CrossRef]
46. Thakur, K.; Kalia, S.; Kaith, B.S.; Pathania, D.; Kumar, A.; Thakur, P.; Knittel, C.E.; Schauer, C.L.; Totaro, G. The development of antibacterial and hydrophobic functionalities in natural fibers for fiber-reinforced composite materials. *J. Environ. Chem. Eng.* **2016**, *4*, 1743–1752. [CrossRef]
47. Jin, F.; Liao, S.; Li, W.; Jiang, C.; Wei, Q.; Xia, X.; Wang, Q. Amphiphilic sodium alginate-polylysine hydrogel with high antibacterial efficiency in a wide pH range. *Carbohydr. Polym.* **2023**, *299*, 120195. [CrossRef]
48. Vityazev, F.V.; Khramova, D.S.; Saveliev, N.Y.; Ipatova, E.A.; Burkov, A.A.; Beloserov, V.S.; Belyi, V.A.; Kononov, L.O.; Martinson, E.A.; Litvinets, S.G.; et al. Pectin-glycerol gel beads: Preparation, characterization and swelling behaviour. *Carbohydr. Polym.* **2020**, *238*, 116166. [CrossRef]
49. Tuyen, N.V.; Ryu, J.H.; Yae, J.B.; Kim, H.G.; Hong, S.W.; Ahn, D.H. Nitrogen removal performance of anammox process with PVA–SA gel bead crosslinked with sodium sulfate as a biomass carrier. *J. Ind. Eng. Chem.* **2018**, *67*, 326–332. [CrossRef]
50. Chen, G.; He, L.; Zhang, P.; Zhang, J.; Mei, X.; Wang, D.; Zhang, Y.; Ren, X.; Chen, Z. Encapsulation of green tea polyphenol nanospheres in PVA/alginate hydrogel for promoting wound healing of diabetic rats by regulating PI3K/AKT pathway. *Mater. Sci. Eng. C* **2020**, *110*, 110686. [CrossRef]
51. Deng, M.-J.; Wu, Y.-S. 2.2 V wearable asymmetric supercapacitors based on Co oxide//Mn oxide electrodes and a PVA-KOH-urea-$LiClO_4$ alkaline gel electrolyte. *J. Alloys Compd.* **2023**, *945*, 169285. [CrossRef]
52. Puguan, J.M.; Yu, X.; Kim, H. Characterization of structure, physico-chemical properties and diffusion behavior of Ca-Alginate gel beads prepared by different gelation methods. *J. Colloid Interface Sci.* **2014**, *432*, 109–116. [CrossRef] [PubMed]
53. Lević, S.; Lijaković, I.P.; Đorđević, V.; Rac, V.; Rakić, V.; Knudsen, T.Š.; Pavlović, V.; Bugarski, B.; Nedović, V. Characterization of sodium alginate/d-limonene emulsions and respective calcium alginate/d-limonene beads produced by electrostatic extrusion. *Food Hydrocoll.* **2015**, *45*, 111–123. [CrossRef]
54. Wang, Y.; Liu, D.; Liao, R.; Zhang, G.; Zhang, M.; Li, X. Study of adhesive self-degrading gel for wellbore sealing. *Colloids Surf. A Physicochem. Eng. Asp.* **2022**, *651*, 129567. [CrossRef]
55. Li, K.; Zhang, B.; Yang, Z.; Jiang, X.; Li, X. Degradation behaviors of silicone gel encapsulation material with moisture intrusion. *Polym. Degrad. Stab.* **2022**, *206*, 110197. [CrossRef]
56. Li, Y.; Shan, P.; Yu, F.; Li, H.; Peng, L. Fabrication and characterization of waste fish scale-derived gelatin/sodium alginate/carvacrol loaded ZIF-8 nanoparticles composite films with sustained antibacterial activity for active food packaging. *Int. J. Biol. Macromol.* **2023**, *230*, 123192. [CrossRef]
57. Li, Q.; Di, J.; Liao, X.; Ni, J.; Li, Q.; He, Y.C.; Ma, C. Exploration of benign deep eutectic solvent–water systems for the highly efficient production of furfurylamine from sugarcane bagasse via chemoenzymatic cascade catalysis. *Green Chem.* **2021**, *23*, 8154–8168. [CrossRef]
58. Ji, L.; Tang, Z.; Yang, D.; Ma, C.; He, Y.C. Improved one-pot synthesis of furfural from corn stalk with heterogeneous catalysis using corn stalk as biobased carrier in deep eutectic solvent-water system. *Bioresour. Technol.* **2021**, *340*, 125691. [CrossRef] [PubMed]
59. Zha, J.; Fan, B.; He, J.; He, Y.C.; Ma, C. Valorization of biomass to furfural by chestnut shell-based solid acid in methyl isobutyl ketone-water-sodium chloride system. *Appl. Biochem. Biotechnol.* **2022**, *194*, 2021–2035. [CrossRef]
60. Shen, J.; Gao, R.; He, Y.C.; Ma, C. Efficient synthesis of furfural from waste biomasses by sulfonated crab shell-based solid acid in a sustainable approach. *Ind. Crops Prod.* **2023**, *202*, 116989. [CrossRef]
61. Gong, L.; Zha, J.; Pan, L.; Ma, C.; He, Y.C. Highly efficient conversion of sunflower stalk-hydrolysate to furfural by sunflower stalk residue-derived carbonaceous solid acid in deep eutectic solvent/organic solvent system. *Bioresour. Technol.* **2022**, *351*, 126945. [CrossRef]

62. Yang, D.; Yang, L.; Li, Q.; Fan, B.; Ma, C.; He, Y.C. Preparation of a biobased polyelectrolyte complex from chitosan and sodium carboxymethyl cellulose and its antibacterial characteristics. *Int. J. Biol. Macromol.* **2023**, *227*, 524–534. [CrossRef]
63. Liu, Y.; Wu, Y.; He, Y.C.; Ma, C. Synthesis of furoic acid from biomasses by sequential catalysis with fish scale-rice husk-based heterogeneous chemocatalyst and dehydrogenase biocatalyst. *Ind. Crops Prod.* **2023**, *202*, 117033. [CrossRef]
64. Tripathi, D.K.; Tripathi, A.; Shweta; Singh, S.; Singh, Y.; Vishwakarma, K.; Yadav, G.; Sharma, S.; Singh, V.K.; Mishra, R.K.; et al. Uptake, accumulation and toxicity of silver nanoparticle in autotrophic plants, and heterotrophic microbes: A concentric review. *Front. Microbiol.* **2017**, *8*, 7. [CrossRef] [PubMed]
65. Cui, J.; Liang, Y.; Yang, D.; Liu, Y. Facile fabrication of rice husk based silicon dioxide nanospheres loaded with silver nanoparticles as a rice antibacterial agent. *Sci. Rep.* **2016**, *6*, 21423. [CrossRef] [PubMed]
66. Ahmed, B.; Hashmi, A.; Khan, M.S.; Musarrat, J. ROS mediated destruction of cell membrane, growth and biofilms of human bacterial pathogens by stable metallic AgNPs functionalized from bell pepper extract and quercetin. *Adv. Powder Technol.* **2018**, *29*, 1601–1616. [CrossRef]
67. Velidandi, A.; Pabbathi, N.P.P.; Dahariya, S.; Baadhe, R.R. Green synthesis of novel Ag–Cu and Ag–Znbimetallic nanoparticles and their in vitro biological, eco-toxicity and catalytic studies. *Nano-Struct. Nano-Objects* **2021**, *26*, 100687. [CrossRef]
68. Zhang, Y.; Dang, Q.; Liu, C.; Yan, J.; Cha, D.; Liang, S.; Li, X.; Fan, B. Synthesis characterization, and evaluation of poly(aminoethyl) modified chitosan and its hydrogel used as antibacterial wound dressing. *Int. J. Biol. Macromol.* **2017**, *102*, 457–467. [CrossRef]
69. Chen, S.; Zhang, Z.; Wei, X.; Sui, Z.; Geng, J.; Xiao, J.; Huang, D. Antibacterial and antioxidant water-degradable food packaging chitosan film prepared from American cockroach. *Food Biosci.* **2022**, *49*, 101893. [CrossRef]
70. Ma, G.; Qian, B.; Yang, J.; Hu, C.; Nie, J. Synthesis and properties of photosensitive chitosan derivatives. *Int. J. Biol. Macromol.* **2010**, *46*, 558–561. [CrossRef] [PubMed]
71. Sun, S.; An, Q.; Qian, L.; He, B.; Xiao, H. Synergistic effects of chitosan–guanidine complexes on enhancing antimicrobial activity and wet-strength of paper. *Bioresour. Technol.* **2010**, *101*, 5693–5700. [CrossRef] [PubMed]
72. Khalaki, M.A.; Moameri, M.; Ghorbani, A.; Alagoz, S.M.; Dolatabadi, N.; Lajayer, B.A.; van Hullebusch, E.D. Chapter 8—Effects, uptake and translocation of Ag-based nanoparticles in plants. In *Toxicity of Nanoparticles in Plants*; Rajput, V.D., Minkina, T., Sushkova, S., Mandzhieva, S.S., Rensing, C., Eds.; Academic Press: Cambridge, MA, USA, 2022; pp. 171–192.
73. Xie, W.; Zhao, K.; Xu, L.; Gao, N.; Zhao, H.; Gong, Z.; Yu, L.; Jiang, J. Oxalic acid cross-linked sodium alginate and carboxymethyl chitosan hydrogel membrane for separation of dye/NaCl at high NaCl concentration. *Chin. Chem. Lett.* **2022**, *33*, 1951–1955. [CrossRef]
74. Xiong, X.; Liu, Z.; Zhao, L.; Huang, M.; Dai, L.; Tian, D.; Zou, J.; Zeng, Y.; Hu, J.; Shen, F. Tailoring biochar by PHP towards the oxygenated functional groups (OFGs)-rich surface to improve adsorption performance. *Chin. Chem. Lett.* **2022**, *33*, 3097–3100. [CrossRef]